APPLIED GEOPHYSICS, Vol.10, No.1 (March 2013), P. 63-70, 7 Figures.
DOI:10.1007/s11770-013-0361-9

A study of damping factors in perfectly matched layers for the numerical simulation of seismic waves*

Yang Hao-Xing[1] and Wang Hong-Xia[1♦]

Abstract: When simulating seismic wave propagation in free space, it is essential to introduce absorbing boundary conditions to eliminate reflections from artificially truncated boundaries. In this paper, a damping factor referred to as the Gaussian damping factor is proposed. The Gaussian damping factor is based on the idea of perfectly matched layers (PMLs). This work presents a detailed analysis of the theoretical foundations and advantages of the Gaussian damping factor. Additionally, numerical experiments for the simulation of seismic waves are presented based on two numerical models: a homogeneous model and a multi-layer model. The results show that the proposed factor works better. The Gaussian damping factor achieves a higher Signal-to-Noise Ratio (SNR) than previously used factors when using same number of PMLs, and requires less PMLs than other methods to achieve an identical SNR.
Keywords: simulation of seismic wave, perfectly matched layer (PML), damping factor

Introduction

Numerical simulations are important for studying seismic wave propagation and pre-stack migration in complex media. In seismic exploration, waves propagate in free space. Because of finite computational resources, it is necessary to truncate the computational area. However, truncation results in artificial reflections from the introduced boundaries. These reflections reduce the Signal-to-Noise Ratio (SNR) of the seismic records and degrade the accuracy of the migration results. In practice, introducing absorbing boundary conditions can efficiently eliminate these reflections without greatly expanding the computational domain.

The PML (perfectly matched layer) (Berenger, 1994) is considered to be the best absorption boundary condition. The key idea of the PML (Hasting et al., 1996) is the construction of absorbing layers outside the computational area to attenuate incident waves at an exponential rate. Because of its excellent absorption over a wide range of incident angles and its insensitivity to frequency, the PML technique has been used extensively in seismic wave modeling (Komatitsch et al., 2003; Wang et al., 2003) and migration (Du et al., 2010).

Damping factors play a key role in the PML technique' s absorption capability. Currently, the most widely used damping factor is the m-power factor proposed by Hasting (1996). He discussed the maximum value of the damping factor in detail and presented the corresponding reflection coefficient based on an anisotropic medium. The study also chose to use a fourth-order scheme to ensure high performance and stability. Wang (2007) applied the m-power damping factor to acoustic wave modeling and presented a corresponding reflection coefficient. Subsequently, Chen (2010) analyzed the disadvantages

Manuscript received by the Editor November 1, 2011; revised manuscript received August 12, 2012.
*The research is supported by the National Natural Science Foundation of China (No. 61072118).
1. School of Science, National University of Defense Technology, Changsha 410073, China.
♦Corresponding Author: Wang Hong-Xia (Email: whx8292@yahoo.com.cn)

of the m-power damping factor and proposed the sine-damping factor. The sine-damping factor's absorption performance was demonstrated by numerical results using a homogeneous model and the Marmousi model. Chen also listed the principles for selecting a damping factor:

1. The damping factor must increase with the propagating distance, so that the absorption capacity can be gradually enhanced.

2. The factor must vary slowly enough to avoid inner reflections caused by numerical discontinuities.

In this paper, first, we review the acoustic wave equation in the PML, derive the equivalent second-order equation and prove its absorption property. Second, we propose the Gaussian damping factor and analyze its properties in comparison with that of other common damping factors. Finally, numerical experiments are used to demonstrate the advantages of the proposed Gaussian damping factor.

PML based absorption boundary condition theory

Independent of the boundary conditions, the key concept of the PML is to place a layer of artificial absorbing material adjacent to the edges of the computation domain. When seismic waves enter the boundary, they are attenuated by this layer and eventually eliminated. In the two-dimensional case, the acoustic wave equation is

$$\frac{1}{v^2}\frac{\partial^2 u}{\partial t^2}=\frac{\partial^2 u}{\partial x^2}+\frac{\partial^2 u}{\partial z^2}, \qquad (1)$$

where $u(\mathbf{x}, t)$ ($\mathbf{x}=(x, z)$) is the seismic wavefield and $v(\mathbf{x})$ is the seismic wave velocity. The first-order PML absorbing boundary condition for acoustic wave equations can be defined as (Collino, 2001; Wang et al., 2007)

$$\begin{aligned}
&\frac{\partial u_x}{\partial t}+\alpha_x u_x=v^2\frac{\partial \xi}{\partial x},\\
&\frac{\partial u_z}{\partial t}+\alpha_z u_z=v^2\frac{\partial \eta}{\partial z},\\
&\frac{\partial \xi}{\partial t}+\alpha_x \xi=\frac{\partial u}{\partial x},\\
&\frac{\partial \eta}{\partial t}+\alpha_z \eta=\frac{\partial u}{\partial z},
\end{aligned} \qquad (2)$$

where u_x and u_z are the components of u along the x-axis and z-axis, respectively, $\xi(\mathbf{x}, t)$ and $\eta(\mathbf{x}, t)$ are the auxiliary wavefields, and $\alpha_x(\mathbf{x})(>0)$ and $\alpha_z(\mathbf{x})(>0)$ are the damping factors along the x-axis and z-axis, respectively. In particular, when assuming $\alpha_x=\alpha_z=\alpha$ and a homogeneous PML medium (i.e., a constant α), the equivalent second-order equation can be shown to equal

$$\frac{\partial^2 u}{\partial t^2}+2\alpha\frac{\partial u}{\partial t}+\alpha^2 u=v^2\left(\frac{\partial^2 u}{\partial x^2}+\frac{\partial^2 u}{\partial z^2}\right). \qquad (3)$$

As the propagation distance increases, the seismic wavefield u is attenuated by the PML and decays at an exponential rate. The damping factor α corresponds to the decay rate. The larger α is, the more rapidly the seismic wave will be attenuated. When $\alpha = 0$， equation (3) degrades to the acoustic wave equation (equation (1)). If $\alpha(\mathbf{x})$ varies slowly, then slight reflections in the PML can be neglected and equation (3) can be applied to a heterogeneous PML. Figure 1 illustrates the arrangement of the PML.

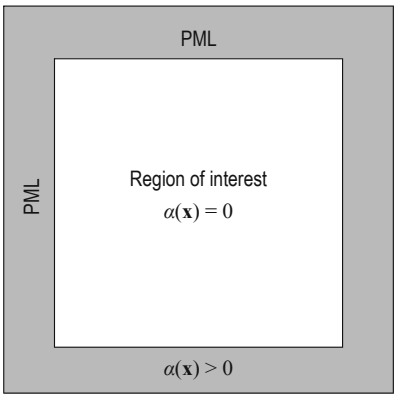

Fig.1 Illustration of the PML arrangement.

In accordance with wave propagation properties, transmission of seismic wave from one material to another causes reflections at the interface, it is necessary to set $\alpha(\mathbf{x}) = 0$ at the interior absorption boundary to ensure that seismic waves completely enter the PML. Next, one must slowly turn on the absorbing capacity of the PML to attenuate seismic waves with slight reflections. This can be accomplished by letting $\alpha(\mathbf{x})$ monotonously increase in the PML, reaching a maximum value at the exterior absorption boundary.

In practice, the PML absorption boundary needs to be discretized. This means that PMLs should be placed with an increasing damping factor from the interior absorption boundary to the exterior boundary. For a given thickness, the absorbing capacity is determined by the properties of the damping factor. Currently, two damping factors are commonly used: the m-power damping factor and the sine-damping factor. The m-power damping factor

(Collino and Tsogka, 2001):

$$\alpha(x) = A\left(\frac{\overline{P_{ML}} - x}{\overline{P_{ML}}}\right)^m, x \in [0, \overline{P_{ML}}], \quad (4)$$

where $\overline{P_{ML}}$ is the thickness of the PML, $x = 0$ indicates the exterior absorption boundary, $x = \overline{P_{ML}}$ indicates the interior absorption boundary, m is the order, and A is the maximum value determined by the reflection coefficient at normal incidence. The reflection coefficient at normal incidence is defined as (Komatitsch and Tromp, 2003)

$$R_\alpha = \exp\left(-\frac{2A\overline{P_{ML}}}{v(m+1)}\right). \quad (5)$$

Chen (2010) defined the sine-damping factor as

$$\beta(x) = A\left(1 - \sin\left(\frac{x\pi}{2\overline{P_{ML}}}\right)\right), x \in [0, \overline{P_{ML}}]. \quad (6)$$

The sine-damping factor's reflection coefficient at normal incidence is

$$R_\beta = \exp\left(-\frac{4A\overline{P_{ML}}}{v\pi}\right). \quad (7)$$

The gradient of the m-power damping factor is

$$\alpha'(x) = -\frac{mA}{\overline{P_{ML}}}\left(\frac{\overline{P_{ML}} - x}{\overline{P_{ML}}}\right)^{m-1}, x \in [0, \overline{P_{ML}}], \quad (8)$$

where m is an experiential parameter. If $m = 1$, then $\alpha(\mathbf{x})$ is linear and not smooth at the interior absorption boundary. This could cause a large numerical discontinuity after discretization on a sparse grid. For larger values of m, $\alpha(\mathbf{x})$ becomes smoother at the interior absorption boundary. However, the gradient of $\alpha(\mathbf{x})$ at the exterior boundary increases. This implies that $\alpha(\mathbf{x})$ excessively increased at the exterior boundary, which is bad for the absorption. Experience shows that setting $m = 4$ usually provides the best absorption results (Hasting et al., 1996). In comparison, the gradient of the sine-damping factor is

$$\beta'(x) = -\frac{\pi A}{2\overline{P_{ML}}}\cos\left(\frac{x\pi}{2\overline{P_{ML}}}\right), x \in [0, \overline{P_{ML}}]. \quad (9)$$

It is smooth and varies slowly on the given interval. These advantages overcome the disadvantages of the m-power damping factor.

Gaussian damping factor

The damping factor has a significant influence on the decay rate. An ideal damping factor has two necessary properties: smoothness at the interior boundary (to allow seismic waves to completely enter the PML), and a low-rate variation in the PML (to prevent large transitions once the PML is discretized).

The Gaussian function can be derived in an arbitrary order. Based on this fact, this paper proposes a new Gaussian damping factor:

$$\gamma(x) = A\left(e^{\left(\frac{\overline{P_{ML}} - x}{\overline{P_{ML}}}\right)^2 \cdot \ln 2} - 1\right), x \in [0, \overline{P_{ML}}]. \quad (10)$$

The reflection coefficient at normal incidence can be computed in a similar manner to the computation in Hasting et al. (1996):

$$\begin{aligned} R_\gamma &= \exp\left(-\frac{2}{v}\int_0^{\overline{P_{ML}}} \gamma(x)dx\right) \\ &= \exp\left(-\frac{2}{v}A\overline{P_{ML}}(\sqrt{15\pi} - 1)\right). \end{aligned} \quad (11)$$

The properties of the proposed Gaussian damping factor are as follows. The gradient of equation (7) is

$$\gamma'(x) = -2\ln 2 \cdot A \cdot \frac{\overline{P_{ML}} - x}{\left(\overline{P_{ML}}\right)^2} e^{\left(\frac{\overline{P_{ML}} - x}{\overline{P_{ML}}}\right)^2 \cdot \ln 2}, \; x \in [0, \overline{P_{ML}}]. \quad (12)$$

Because $\gamma'(\overline{P_{ML}}) = 0$, the smoothness property is satisfied.

For simplicity, let $\overline{P_{ML}} = 1$ and $A = 1$. Figure 2 and Table 1 show the properties of the three factors (m-power, sine, and Gaussian). Figure 2a shows plots of the factors and Figure 2b shows plots of the factor gradients ($m = 4$). Table 1 lists the values of the gradients at $x = 0$, 1/3, 1/2, and 1.

Table 1 Comparison of the damping factor gradients

	$x = 0$	$x = 1/3$	$x = 1/2$	$x = 1$
m-power	-4	-1.6875	-0.6655	0
Sine	-1.5707	-1.4512	-1.1944	0
Gaussian	-2.7726	-1.5354	-0.9403	0

Figure 2b and Table 1 show that all gradients are zero at $x = 1$ and that all factors are smooth,

respectively. However, at $x = 1/2$, the gradient of the m-power damping factor is smaller and its value at the exterior boundary ($x = 0$) is much larger than the values of the other damping factors. This implies that the m-power damping factor varies much faster around the exterior boundary and is more likely to cause reflections on sparse grids. In comparison, the sine-damping factor and the Gaussian damping factor perform better at the exterior boundary.

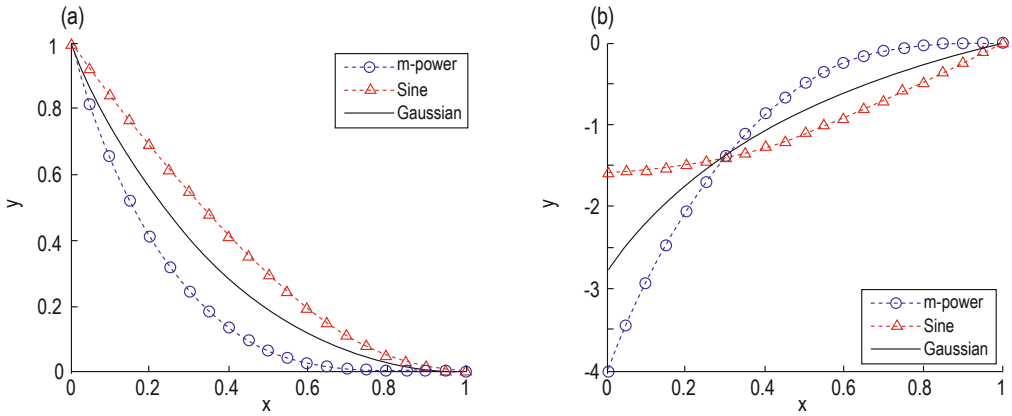

Fig.2 Plots of the damping factors (a) and the factor gradients (b).

A pseudo-spectral method

The simulation region shown in Figure 1 can be divided into two parts: the region of interest and the PML region. In the region of interest, the seismic wavefield is the solution of the acoustic wave equation (equation (1)), whereas, in the PML region, the seismic wavefield equation becomes equation (3). To numerically evaluate the nonreflecting solution, the problem needs to be discretized. This paper uses the pseudo-spectral method to solve the problem, which involves spectral differentiation in the spatial domain and forward marching in the time domain. This can efficiently guarantee the accuracy in spatial domain and suppress numerical dispersion. In the region of interest, the second-order central difference scheme is

$$u^{n+1} = 2u^n - u^{n-1} - \Delta t^2 v^2 [F^{-1}(k_x^2 + k_z^2)F]u^n, \quad (13)$$

where F is the two-dimensional Fourier transform operator and F^{-1} is its inverse. In the PML region, equation (13) is discretized to have:

$$u^{n+1} = \frac{1}{1+\alpha\Delta t}\{(2-\alpha^2\Delta t^2)u^n - (1-\alpha\Delta t)u^{n-1} - \Delta t^2 v^2 [F^{-1}(k_x^2 + k_z^2)F]u^n\}. \quad (14)$$

Next, it is necessary to discretize the dampling factors. The discretized form of the Gaussian factor is

$$\gamma_i = A\left(e^{\left(\frac{P_{ML}-i}{P_{ML}}\right)^2 \cdot \ln 2} - 1\right), i = 0,1,\ldots,P_{ML}, \quad (15)$$

where P_{ML} is the total number of grid points occupied by the P_{ML}, and i is the grid point index (i = 0 at the exterior absorption boundary and $i = P_{ML}$ at the interior absorption boundary). Take the left PML boundary as an example. Equation (14) can be further discretized to

$$u_{j,k}^{n+1} = \frac{1}{1+\gamma_j\Delta t}\{(2-\gamma_j^2\Delta t^2)u_{j,k}^n - (1-\gamma_j\Delta t)u_{j,k}^{n-1} - \Delta t^2 v_{j,k}^2 [F^{-1}(k_x^2 + k_z^2)F]u_{j,k}^n\}$$

$$j = 0,1,\ldots,P_{ML}. \quad k = 0,\ 1,\ \ldots,\ nz. \quad (16)$$

where j and k represent the x-axis and the z-axis coordinates, respectively, and nz is the total number of grid points along the z-axis. The discretization process is similar for the m-power damping factor and the sine-damping factor.

Numerical experiments

Numerical experiments were conducted to verify the efficiency of the Gaussian damping factor in this section.. The first experiment uses a homogeneous medium with a seismic wave velocity of 2000 m/s. The model scale

is 200×200 and the spacing intervals Δx and Δz are 20 m. The time interval Δt is 2 ms. The source is motivated by a Ricker wavelet with a maximum frequency of 20 Hz. To compare the absorption performance of the three factors, the first experiment applies a special PML design that is shown in Figure 3. The top and bottom absorption boundaries use the Gaussian damping factor. The left absorption boundary uses the sine damping factor, and the right absorption boundary uses the m-power damping factor ($m = 4$). The parameter A in equation (8) is computed using the reflection coefficient and the four absorption boundaries have an identical thickness.

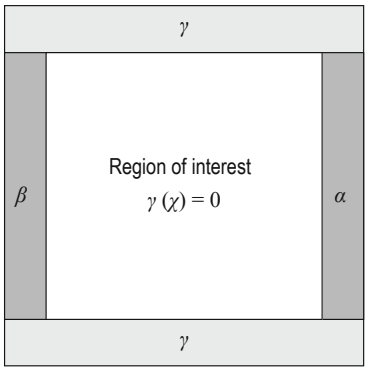

Fig. 3 Construction of the PMLs.

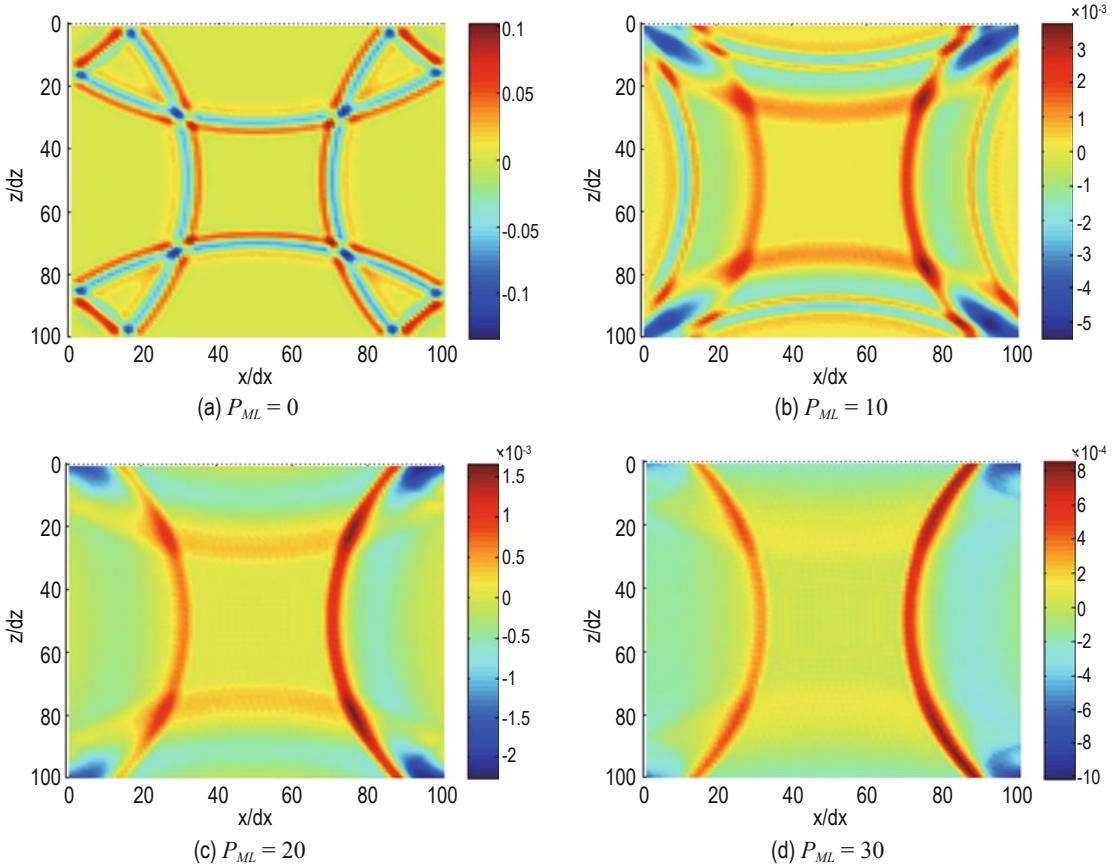

Fig.4 Wavefield snapshot of model with a homogeneous medium.

Figure 4 shows wavefield snapshots at $t = 0.84$ s for different values of P_{ML}. Figure 4a – 4d correspond to $P_{ML} = 0$, 10, 20, and 30, respectively. Figure 4a is the unabsorbed result; reflections are strong and the amplitude reaches 10^{-1}. The use of PMLs causes the reflections to attenuate rapidly. For $P_{ML} = 10$ the amplitude of the reflections is reduced to 10^{-3} or lower (Figure 4b). For increasing values of P_{ML}, the absorption effect gradually improves. For $P_{ML} = 30$, the maximum amplitude of the reflections is less than 10^{-3}.

By comparing the wavefield behavior near the four boundaries, we find that the sine-damping factor has a better absorption performance than the m-power damping factor and a worse absorption performance than the Gaussian damping factor. For example, in Figure 4d, the reflections from the up and down boundaries, whose maximum amplitude is less than 10^{-4}, are weaker than the reflections from the left and right boundaries. This demonstrates that the proposed factor can better constrain artificial reflections from the truncated boundaries, resulting in more accurately modeled wavefields.

To qualitatively investigate the absorption effects of

the Gaussian damping factor, the second experiment is based on a multi-layer model shown in Figure 5. The acoustic source is the same as the first experiment. The numbers of grid points along the x and z axes are 200 and 100, respectively. The step size is $\Delta x = \Delta z = 20$ m. At the same time, the time interval is uniformly discretized into 700 grids with step size $\Delta t = 2$ ms.The source is located at (2000 m, 0 m), Figure 1 shows the construction of the PMLs, which have an identical damping factor and thickness. Figure 6a presents the unabsorbed single shot record, Figure 6b presents the record obtained with the m-power damping factor, Figure 6c presents the record obtained with the sine-damping factor, and Figure 6d presents the record obtained with the Gaussian damping factor. In the unabsorbed record (Figure 6a), there are strong reflections from the truncated boundaries. These reflections are greatly attenuated in Figures 6b and 6c, and are increasingly attenuated in Figure 6d, which is almost identical to the nonreflecting record obtained by enlarging the computational domain. This demonstrates that, in the multi-layer model, the Gaussian damping factor has a better performance than the other two factors (for an identical P_{ML}).

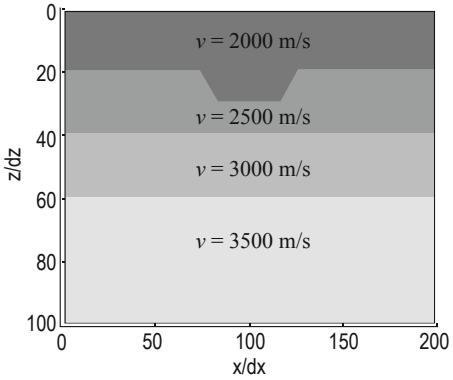

Fig.5 Multi-layer model.

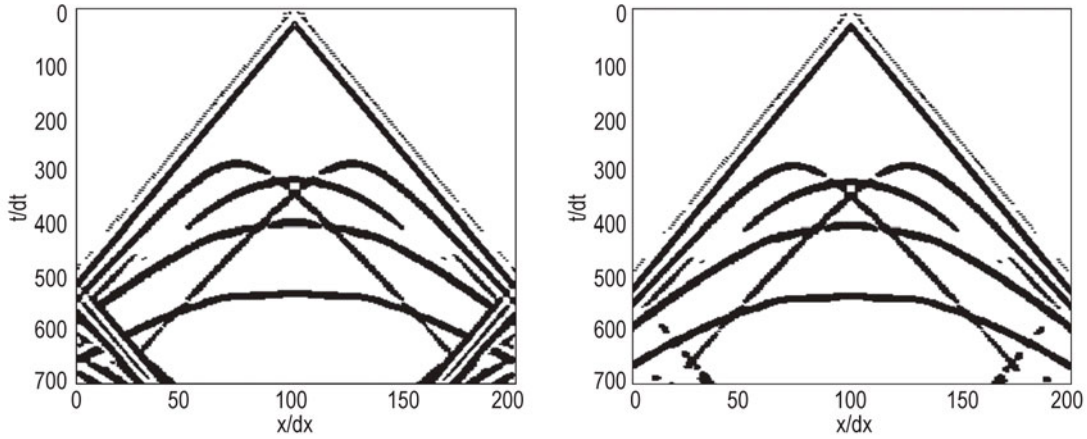

(a) Unabsorbed record. (SNR = 11.33 dB)

(b) Record obtained with the m-power absorption factor. (P_{ML} = 10, SNR = 34.38 dB)

(c) Record obtained with the sine-absorption factor. (P_{ML} = 10, SNR = 37.53 dB)

(d) Record obtained with the Gaussian absorption factor. (P_{ML} = 10, SNR = 38.17 dB)

Fig. 6 Single shot records.

Because artificial reflections can be regarded as regular noise, a SNR is introduced to quantitatively evaluate the absorbing results as follows:

$$\mathrm{SNR} = 10\lg\frac{\|P_{signal}\|^2}{\|P_{noise}\|^2}, \qquad (17)$$

where P_{signal} denotes the nonreflecting record and is obtained by extending the computational domain, and P_{noise} denotes the difference between the record obtained with the PML absorbing boundary condition and the nonreflecting record. The SNR represents the energy difference between records with and without reflections. A large SNR implies the record contains little reflection. Figure 7 presents SNR plots of the seismic records obtained with different damping factors. Table 2 presents part of the SNR data.

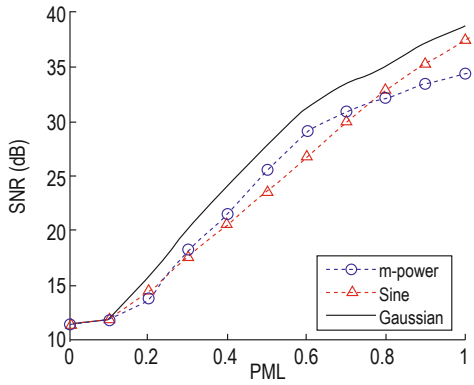

Fig.7 Plots of SNR for different values of P_{ML}.

Table 2 Comparison of the SNR (dB) on different situations

Factor	$P_{ML}=2$	$P_{ML}=4$	$P_{ML}=6$	$P_{ML}=8$	$P_{ML}=10$
m-power	13.64	21.43	29.11	32.17	34.39
Sine	14.34	20.51	26.77	32.84	37.53
Gaussian	15.64	23.92	31.30	34.90	38.17

In Figure 7 and Table 2, the SNR plots monotonically increase, showing that the reflections degrade as the P_{ML} increases. For values of P_{ML} larger than or equal to 8, the SNR of the records is larger than 30 dB. The SNR plot obtained with the Gaussian damping factor is above the other plots, showing that the Gaussian damping factor performs better than the other factors with respect to the SNR. For value of P_{ML} less than or equal to 8, the sine-absorption factor is not better than the m-power absorption factor with respect to the SNR. For value of $P_{ML}>8$, the sine-absorption factor is much better than the m-power absorption factor. For identical P_{ML} values, the Gaussian damping factor is better at eliminating reflections than the other factors. Additionally, for identical SNRs, the Gaussian damping factor requires less PMLs in comparison to the other factors. However, Gaussian and Sine factor SNR curve tends to be close as P_{ML} increases.

Additionally, for identical SNRs, the Gaussian damping factor requires less PMLs in comparison to the other factors.

Conclusions

This paper proposed a damping factor referred to as the Gaussian damping factor. The properties of the Gaussian damping factor and the sine type absorption factor, and types of power function were analyzed and compared. Numerical experiments with a homogeneous model and a multi-layer model were presented, and showed that the Gaussian damping factor yielded a higher SNR and only required fewer PMLs. Because it is difficult to theoretically prove the advantages of the proposed factor, we evaluated the factor based on its properties and its performance in numerical experiments. The idea used in the construction of Gaussian factor is also helpful to derive other PML factors in wave equations. Because of the extensive application of PML absorbing boundary conditions in seismology, the results of this paper can be used to obtain relatively accurate data in numerical modeling, migration, and inversion.

References

Berenger, J. P., 1994, A perfectly matched layer for the absorption of electromagnetics waves: Journal Computation Physics, **114**, 185 – 200.

Burns, D. R., 1992, Acoustic and elastic scattering from seamounts in three dimensions-numerical modeling study: J. Acoust. Soc. Amer., **92**, 2784 – 2791.

Cerjan, C., Kosloff, D., Kosloff, R., and Reshef, M., 1985, A nonreflecting boundary condition for discrete acoustic and elastic wave equations: Geophysics, **50**(4), 705 – 708.

Clayton, R., Engquist, B., 1977, Absorbing boundary condition for acoustic and elastic wave equations: Bull. Sersm. Soc. Am., **67**, 1529 – 1540.

Collino, F., and Tsogka, C., 2001, Application of the perfectly matched absorbing layer model to the linear elasto-dynamic problem in anisotropic heterogeneous

media: Geophysics, **66**(1), 294 – 307.

Du, Q. Z., Sun, R. Y., Qin, T., Zhu, Y. T., and Bi, L. F., 2010, A study of perfectly matched layers for joint multicomponent reverse-time migration: Applied Geophysics, **7**(2), 166 – 173.

Hastings, F., Schneider, J. B., and Broschat, S. L., 1996, Application of the perfectly matched absorbing layer (PML) absorbing boundary condition to elastic wave propagation: Journal of Acoustic Society of America, **100**(5), 3061 – 3069.

Higdon, R. L., 1986, Absorbing boundary conditions for difference approximations to the multidimensional wave equation: Math. Comp., **47**, 437 – 459.

Higdon, R. L., 1987, Numerical absorbing boundary conditions for the wave equation: Math. Comp., **49**, 65 – 90.

Higdon, R. L., 1991, Absorbing boundary condition for elastic waves: Geophysics, **56**(2), 231 – 241.

Komatitsch, D., Tromp, J., 2003, A perfectly matched layer absorbing boundary condition for the second-order seismic wave equation: Geophysical Journal International, **154**(1), 146 – 150.

Liao, Z. P., Wong, H. L., Yang, B. P., and Yuan, Y. F., 1984, A transmitting boundary for transient wave analysis: Scientia Sinica (Series A), **27**(10), 1063 – 1076.

Wang, T., and Tang, X. M., 2003, Finite-difference modeling of elastic wave propagation: a nonsplitting perfectly matched layer approach: Geophysics, **68**(5), 1749 – 1755.

Wang, Y. G., Xing, W. J., Xie, W. X., and Zhu, Z. L., 2007, Study of absorbing boundary condition by perfectly matched layer: Journal of China University of Petroleum (In Chinese), **31**(1), 19 – 24.

Yang Hao-Xing received his B.S. in Applied Mathematics from the National University of Defense Technology of China (NUDT). He is now a graduate student at the Department of Mathematics and System Science of NUDT. His research interests are mainly about the computational problems in reverse time migration of seismic data.

Wang Hong-Xia received her Ph.D. in Computational Mathematics from NUDT in 2004 and then held a postdoctoral researcher position in the Institute of Computational Mathematics and Scientific/Engineering Computing of Chinese Academy of Sciences from November 2005 to October 2007. Now she is visiting the Courant Institute of Mathematical Sciences. Her research interests include multi-scale analysis, image processing, seismic data imaging and high-dimensional data analysis.